IEEE Access
Multidisciplinary | Rapid Review | Open Access Journal

Received December 24, 2019, accepted February 9, 2020, date of publication February 18, 2020, date of current version February 27, 2020.

Digital Object Identifier 10.1109/ACCESS.2020.2974912

A New Model to Determine Effective Permittivity and Resonant Frequency of Patch Antenna Covered With Multiple Dielectric Layers

DINESH RANO[1], (Student Member, IEEE),
MUHAMMAD A. CHAUDHARY[2], (Senior Member, IEEE),
AND MOHAMMAD S. HASHMI[1,3], (Senior Member, IEEE)

[1]Department of Electronics and Communication Engineering, Indraprastha Institute of Information Technology Delhi (IIIT Delhi), New Delhi 110020, India
[2]Department of Electrical and Computer Engineering, Ajman University, Ajman, United Arab Emirates
[3]Department of Electrical and Computer Engineering, Nazarbayev University, 010000 Nur-Sultan, Kazakhstan

Corresponding author: Dinesh Rano (dineshr@iiitd.ac.in)

This work was supported by the Media Lab Asia (Ministry of Electronics and IT, India) through the Visvesvaraya Ph.D. Fellowship.

ABSTRACT This paper reports a model to determine effective permittivity (ε_{eff}) and resonant frequency (f_r) of microstrip patch antenna (MPA) covered with multiple dielectric layers. This model is augmented with a newly developed empirical expression to determine the ε_{eff} of multi-layered superstrates over a substrate. The development of empirical formulation makes use of conformal mapping approach (CMA) and series–parallel combination of dielectric boundaries between the ground plane and patch of the MPA. In this work, the MPA is designed on substrate having dielectric constant of ε_1 whereas the superstrate layers have dielectric constants of ε_2, $\varepsilon_3 \ldots \varepsilon_n$. It is shown that the proposed technique is able to predict the f_r of MPA with error of 1.8%, 3.5%, and 1.4% when it is covered with a single dielectric layer with superstrate height of 4.5mm for respective conditions of $\varepsilon_1 = \varepsilon_2$, $\varepsilon_1 > \varepsilon_2$ and $\varepsilon_1 < \varepsilon_2$ ($\varepsilon_1 = 3.66$, $\varepsilon_2 = 2.2/4.7$). Furthermore, the developed technique is analyzed for distinct combination of substrate and two superstrate layers for the cases $\varepsilon_1 = \varepsilon_2 > \varepsilon_3$, $\varepsilon_1 = \varepsilon_2 < \varepsilon_3$, $\varepsilon_1 < \varepsilon_2 > \varepsilon_3$, $\varepsilon_1 > \varepsilon_2 < \varepsilon_3$, and $\varepsilon_1 > \varepsilon_2 > \varepsilon_3$. Subsequently, the viability of the proposed technique is demonstrated in practical scenarios for body centric communications by considering single (e.g., jeans cotton, pure cotton, rayon, polyester, felt fabric, terry wool, and leather) and multiple (e.g., wool over jeans cotton and polyester, felt fabric over pure cotton and rayon) layers of textiles over MPA. The measurement results on various dielectric superstrates and textiles show excellent agreement with the corresponding theoretical results and thereby validate the reported theory. Finally, a comparison with the seminal works clearly shows the promise of the reported technique in this paper.

INDEX TERMS Body centric communication, conformal mapping (CM), conformal mapping approach (CMA), filling fraction, microstrip patch antenna (MPA), superstrate.

I. INTRODUCTION

MPAs possess low profile, light weight, and compact size and therefore find usefulness in myriad of communication applications such as hand held portable radio, mobile equipment, and IOT sensor [1]–[5]. Numerous applications often have antennas below dielectric layers for protection against environmental hazards and as a consequence the effective dielectric constant (ε_{eff}) of the MPAs covered with layers get altered significantly. Such scenarios shift the original resonant frequency (f_r) and hence lead to the out of band communication considering that MPAs exhibit narrow fractional bandwidth (2–3%) [6]–[7]. The body centric communication sensors are ready example of such a situation in which transmission happens through multiple layers of textiles and are adversely impacted due to multiple layers over MPAs [8]–[11]. This issue can be addressed by determining ε_{eff} and shifts in the f_r apriori. A literature survey reveals that a

The associate editor coordinating the review of this manuscript and approving it for publication was Yasar Amin.

number of techniques have been reported earlier and these include the complex methods namely variational, spectral, modified Wolff model, the full wave analysis, and the conformal mapping (CM) based techniques [12]–[22].

The comparison of the measured and theoretical f_r of the MPA covered with superstrates of permittivity 2.32, 2.6, and 3 for relatively thinner height exhibit errors of more than 4%, 4.5%, and 2.3% in the variational method [12]. On the other hand, the spectral domain approach achieves very good accuracy in predicting f_r and the input impedance for similar configurations. However, this accuracy is for higher order mode, TM_{12} [13]. The modified Wolff model achieves accuracy of 0.5% w.r.t. measured results for relatively thicker heights. However, the report only exist for fewer superstrates and that too for substrates having identical dielectric constants [14]–[15]. The modified Wolff model suffers from serious limitations because in the first step it computes the real input impedance of MPA covered with multiple layers and then determines the modified f_r. It leads to large shift in f_r due to propagation of error to successive stages. All these techniques, although, can determine f_r with reasonable accuracy but at the cost of high computational time and therefore find limited usefulness in integration with standard microwave simulators [19]–[21]. The CM based technique with simpler closed form expressions, although rely on approximation, can predict f_r of superstrate covered MPA with almost similar accuracy and is also compatible with software tools such as MATLAB [19]–[20]. For example, a square MPA covered with a dielectric, this technique can predict f_r with error of 0.22% which is better to variational method (2%) and modified Wolff model (0.89%) [19]. However, it has been observed that the CM based models exhibit higher error between the theoretical and measured f_r for superstrate of $\varepsilon_r > 3$. Therefore, the existing techniques are often constrained in emerging biomedical and e-health related applications as mentioned in the following points.

- A CM based technique uses quasi-static model to determine ε_{eff} for microstrip line covered with multi-layers of superstrate [21]. However, these are not good to compute ε_{eff} and f_r for MPA covered with multiple dielectric layers.
- The existing approach ignores the material present above the air gap for the determination of ε_{eff} and f_r [20]. This essentially means that the MPA is radiating into the infinitely thick spaced superstrate rather than the free space. However, such a scenario is highly unlikely in practice and hence the height of subsequent superstrate layers need to be taken into account in the determination of ε_{eff} and f_r.
- The existing approaches have only analyzed the situation of superstrate covered MPA for substrate with permittivity smaller than 2.47 [12]–[20]. However, MPA designed on substrate with permittivity larger than 2.47 and covered with textiles are often used in dresses and clothes and thereby the techniques are not able to fulfill the current needs.

We had proposed a preliminary work based on CMA to address some of the above concerns [22]. This paper significantly expands the work and proposes following contributions to advance state-of-the-art [19]–[21].

- Development of a new empirical relation to determine ε_{eff} of MPA covered with superstrate layer. It makes use of CM and equivalent capacitance between the metallic plates partially covered by dielectric layers. It exhibits superior performance w.r.t. earlier reported CM based techniques.
- Development of a unique iterative model to determine ε_{eff} and f_r of MPA covered with either single or multiple layers of dielectric. It uses modified relation (in point *a*) in each iteration to determine ε_{eff} of the overall geometry. The earlier approaches (either numerical or CMA) evaluated ε_{eff} by substituting the total thickness of the superstrate in the expression and it is the fundamental drawback of these techniques. The proposed technique, on the other hand, allows fragmentation of multiple superstrate layers over the MPA to separately determine ε_{eff} and f_r.
- The proposed method allows to consider the thickness of the dielectric over a spaced MPA. Furthermore, the proposed method also allows to restore the original f_r of MPA covered with dielectric layers by modifying its physical parameters.

The validation of the proposed method is carried out by designing MPAs operating at 2.38 GHz on substrate (ε_1) RO4350B and FR4. It is then investigated with covering of several superstrate layers such as RO4350, RO5880, FR4, cotton, wool, rayon etc. First, the model and the formulation is analyzed by combining two superstrate layers namely RO5880 (ε_3) over RO4350B (ε_2), FR4 (ε_3) over RO4350B (ε_2). Subsequently, the investigation is repeated for multiple combinations such as $\varepsilon_1 = \varepsilon_2 > \varepsilon_3$, $\varepsilon_1 = \varepsilon_2 < \varepsilon_3$, $\varepsilon_1 < \varepsilon_2 > \varepsilon_3$, $\varepsilon_1 > \varepsilon_2 < \varepsilon_3$, and $\varepsilon_1 > \varepsilon_2 > \varepsilon_3$. During investigation, an intermediate permittivity ($\varepsilon_{\text{effi}}$) of the first superstrate and substrate is computed and then $\varepsilon_1 = \varepsilon_{\text{effi}}$ is taken to determine the overall ε_{eff} of the whole structure. Finally, extensive analysis for the MPA covered with multiple layers of textiles such as *felt fabric* over *pure cotton* and *rayon*, *terry wool* over *jean cotton* etc. that mimic typical scenarios of sensors in body centric communication is also carried out. The theoretical analysis is then augmented with CST simulation results to expedite the verification of the proposed technique. The use of commercially available antenna simulator allows study of number of cases (with multiple substrate/superstrate thicknesses) without any prototyping of all those test cases. The proposed technique is then benchmarked against the well-known CM based techniques [19]–[21].

It is imperative to mention that the proposed model, even though iterative, allows determination of resonant frequency in very short time in comparison to standard simulation software tool such as CST which relies on mesh settings for higher accuracy. For example, an antenna designed on RO4350B, with height of 1.524mm and permittivity of 3.66,

and covered with identical layer of dielectric takes 5 and 4.3 minutes for mesh cells of around 280,000 on i5 and i7 processors respectively in CST. For this case, the proposed model takes around 1.2s with a nominal error of 0.2% w.r.t. simulation in MATLAB (described in section IV). The mesh cells and simulation time will drastically increase for complex designs like antenna array, conformed antenna, and MPA covered with multiple or thick dielectric layers [23]. Furthermore, to restore the original f_r of the dielectric covered MPA, backtracking approach to modify the dimension of the MPA has to be adopted which further increases the simulation time in any standard simulator. Interestingly for the proposed approach, substitution of the determined effective permittivity in the standard expression results in modified dimensions. This effectively reduces the simulation time and leads to the expedited design process.

Section II presents the formulation of the modified closed form expressions to determine ε_{eff} based on series–parallel combination of capacitances between the metallic layers of the patch and the ground plane. Section III explains the iterative model and a MATLAB compatible algorithm. Section IV includes the analysis of the developed technique for single layered superstrate structures along with the textiles whereas section V provides the development of model for two superstrate structures over the MPA. The section VI compares the theoretically obtained results with the measured results while section VII concludes the paper.

II. FORMULATION OF EFFECTIVE PERMITTIVITY FOR SINGLE SUPERSTRATE LAYER OVER MPA

An MPA designed on substrate with permittivity ε_1, region shaded in brown, and height h having length and width of W and L respectively is shown in Fig. 1. It is covered by a superstrate layer of permittivity ε_2 and height $h_2 - h$, the region shaded in red. For $W/h > 1$, CM is applied at the two interfaces namely substrate (ε_1)/superstrate (ε_2) and superstrate (ε_2)/air (ε_o) using Wheeler's transformation [17]–[18]. It means that the angle of refraction at the interfaces ($x - y$) must be retained while conforming the dielectric boundaries to complex flux–potential plane shown in Figs. 2(a)–(b). The terms q_0, q_1, and q_2 are the effective filling fractions of air, substrate, and superstrate boundaries defined by ratio of area occupied by a given dielectric ($S_{\varepsilon 1}$, $S_{\varepsilon 2}$, $S_{\varepsilon o}$) to overall area (S). For example, q_1 is given by ratio of area for the substrate, $S_{\varepsilon 1}$ and the whole area, S, in the W-plane [18]. The overall filling fraction, q, in terms of q_0, q_1, and q_2 is expressed in (1).

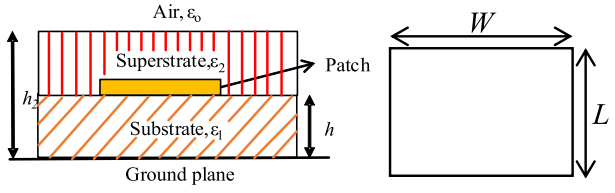

FIGURE 1. MPA with dimensions W and L covered with a single superstrate layer.

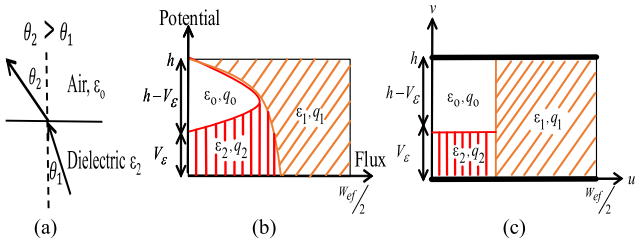

FIGURE 2. (a) Refraction of EM wave travelling from a dielectric medium to air (Snell's law) [θ_1 and θ_2 are incident and refracted angles of EM wave] (b) Conformed dielectric boundaries in flux-potential plane (W-plane) (Shaded portions indicates: red–superstrate, brown–substrate, and white-air), (c) Approximation of dielectric boundaries q_0 and q_2 with associated permittivities.

Therefore q, q_0, q_1, and q_2 in terms of S, $S_{\varepsilon 0}$, $S_{\varepsilon 1}$, and $S_{\varepsilon 2}$ is expressed in (2). Since $S_{\varepsilon 1} + S_{\varepsilon 2} + S_{\varepsilon 0} = S$, q in (2) reduces to unity. Moreover, the dielectric boundaries of q_2 and q_0, as shown in Fig. 2b, can be approximated in the form shown in Fig. 2c [18].

$$q = q_1 + q_2 + q_0 \tag{1}$$

$$q = \frac{S_{\varepsilon 1}}{S} + \frac{S_{\varepsilon 2}}{S} + \frac{S_{\varepsilon 0}}{S} = \frac{S_{\varepsilon 1} + S_{\varepsilon 2} + S_{\varepsilon 0}}{S} \tag{2}$$

This work uses the expressions for filling fractions q_0, and q_1 for an MPA with width, W, given in [18]. However, expression of q_2 has some inconsistency for $h_2 = h$ and hence makes use of expression (3) to include this case [20]. Moreover, the effective width of the patch that takes into account the fringing at the edges, W_{ef}, and the extent of superstrate layer in imaginary axis of W-plane, V_ε, depicted in Figs. 2(b)–(c) are expressed in (4) – (5) [18].

$$q_{2\text{new}} = 1 - q_1 - q_0 - \frac{h}{2W_{ef}} \ln\left[\frac{\pi}{2} - \frac{h}{2W_{ef}}\right] \tag{3}$$

$$W_{ef} = W + \frac{2h}{\pi} \ln\left[17.08\left(\frac{W}{2h} + 0.92\right)\right] \tag{4}$$

$$V_\varepsilon = \frac{2h}{\pi} \tan^{-1}\left[\frac{\pi}{\frac{\pi}{2}\frac{W_{ef}}{h} - 2}\left(\frac{h_2}{h} - 1\right)\right] \tag{5}$$

Furthermore, the respective capacitance per unit area of the substrate regions, $S_{\varepsilon 1}$, $S_{\varepsilon 0}$, and $S_{\varepsilon 2}$, can be expressed as $C_1 = (\varepsilon_1 q_1)/h$, $C_0 = (\varepsilon_0 q_0)/h_1$, and $C_2 = (\varepsilon_2 q_{2\text{new}})/V_\varepsilon$. Here, $h_1 = h - V_\varepsilon$. The series equivalent capacitance, C_{eqs}, between C_0 and C_2 is expressed in (6) and hence the equivalent capacitance, C_{eff}, of the arrangement in Fig. 2(c) consists of parallel combination of C_1 and C_{eqs} is expressed in (7). The expressions (6)–(7) can be simplified using C_1 to get (8). This effective capacitance in terms of effective permittivity, ε_{eff}, the overall filling fraction, q, and the total height of the arrangement, h_2, is then expressed by (9). Finally, (1), (8)–(9) can be used to obtain expression for ε_{eff} in (10) [22]. Further simplification ε_{eff} in (11) is achieved by making use of ε_{eqs} given in (12).

$$C_{\text{eqs}} = \frac{\varepsilon_2 q_{2\text{new}} \varepsilon_0 q_0}{\varepsilon_2 q_{2\text{new}} h_1 + \varepsilon_0 q_0 V_\varepsilon} \tag{6}$$

$$C_{\text{eff}} = C_{\text{eqs}} + C_1 \tag{7}$$

$$C_{\text{eff}} = \frac{\varepsilon_2 q_{2\text{new}} \varepsilon_0 q_0}{\varepsilon_2 q_{2\text{new}} h_1 + \varepsilon_0 q_0 V_\varepsilon} + \frac{\varepsilon_1 q_1}{h} \tag{8}$$

$$C_{\text{eff}} = \frac{\varepsilon_{\text{eff}} q}{h_2} \tag{9}$$

$$\varepsilon_{\text{eff}} = \frac{\varepsilon_1 q_1 h_2}{h} + \frac{\varepsilon_2 q_{2\text{new}} \varepsilon_0 q_0 h_2}{\varepsilon_2 q_{2\text{new}} h_1 + \varepsilon_0 q_0 V_\varepsilon} \tag{10}$$

$$\varepsilon_{\text{eff}} = \frac{\varepsilon_1 q_1 h_2}{h} + \varepsilon_{\text{eqs}} \tag{11}$$

$$\varepsilon_{\text{eqs}} = \frac{\varepsilon_2 q_{2\text{new}} \varepsilon_0 q_0 h_2}{\varepsilon_2 q_{2\text{new}} h_1 + \varepsilon_0 q_0 V_\varepsilon} \tag{12}$$

It can be inferred from (11) and (12) that the known values of ε_0, ε_1, ε_2, h, h_2 and the computed values of W_{ef}, V_ε, q_0, q_1, $q_{2\text{new}}$ can enable the determination of ε_{eff} of the combination of layers depicted in Fig. 1. Apparently, this proposed formulation takes into account the height of the single superstrate layers and therefore aid in the accurate determination of ε_{eff} unlike the technique reported in [20]. Furthermore, the proposed formulation and the model proposed here to determine ε_{eff}, although is based on CM, is distinct from the seminal work in [19]–[20].

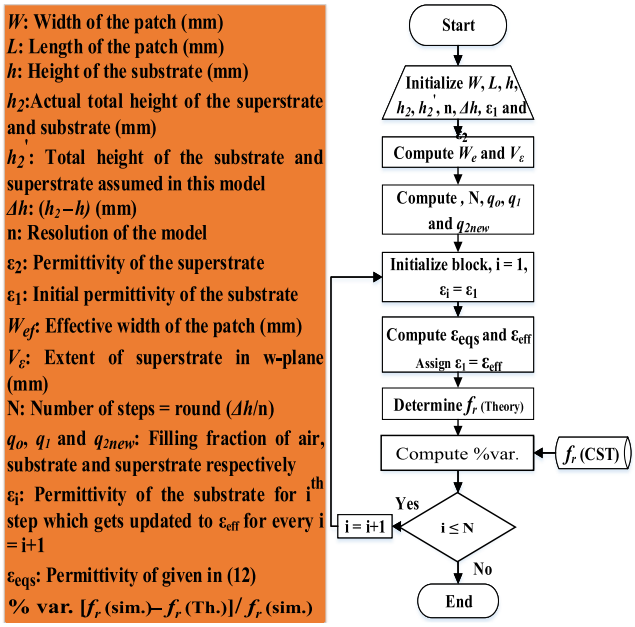

FIGURE 3. Proposed model to determine effective permittivity of MPA covered with single superstrate layer (simulations are performed on CST software).

III. PROPOSED MODEL FOR SINGLE SUPERSTRATE LAYER

The flow chart depicted in Fig. 3 includes all the steps involved in the calculation of ε_{eff} and f_r of the MPA shown in Fig. 1. It is important to mention that the proposed model does not take into account the theoretically obtained length of the MPA rather it considers the optimized simulated values unlike the seminal works [19]–[20]. This is because theoretically obtained length and width of the MPA for a given f_r assumes ground plane and substrate is of infinite extent. However, practical MPAs always have finite dimensions of ground plane and substrate and hence the antenna designed with these values in simulation software (CST) often show shift from the actual f_r. Apparently, the design of MPA on a given substrate is the first step followed by covering of dielectric layer, all the physical parameters of MPA are independent of cover characteristics. Following steps which explain the flow chart is analyzed using MATLAB.

Step 1: Choose the substrate, superstrate, and antenna's parameters such as height, permittivity, length, and width. Here, actual superstrate's height is $\Delta h = h_2 - h$ from Fig. 1. The total height of the substrate and the superstrate is taken as h_2' given by $h_2' = h + n$. As a consequence, h_2 in (5), (9)-(12) is replaced by h_2'. The superstrate layer in this model is divided into 'N' smaller blocks of thickness 'n' each. Selection of n is explained using an example whereas selection of N is elaborated in step 3. Say, an MPA designed on substrate RO4350B of permittivity and height of 3.66 and 1.524mm is covered by a dielectric identical to the substrate. This makes $h_2' = 1.524 + n$ mm. For $n = 0.1$ mm, $\varepsilon_{\text{eff}} = 3.679$ using (3)–(12). For any smaller n, say 0.09 or 0.08 mm, the value of ε_{eff} is smaller than 3.66. Thus, n assumes the limiting value for which ε_{eff} is just greater than ε_1. It is obvious that for larger n, say 0.11 mm or any other value, the ε_{eff} will be greater than ε_1 but due to iterative nature of the model the value becomes impractically larger for thicker superstrates. As a simple rule, n starts from 0.01 and ends at the value for which $\varepsilon_{\text{eff}} > \varepsilon_1$ with step size of 0.01. It is important to note that the selection of n is not part of the main algorithm and is therefore not part of the flow chart in Fig. 3.

Step 2: Use the parameters from step 1 to determine the values of W_{ef} and V_ε using (4)–(5).

Step 3: Compute the filling fractions q_o, and q_1, using expressions in [20]. Use (3) to calculate q_{2new}. In addition, also compute number of steps N using round ($\Delta h/n$) to find the maximum iterations (no. of blocks) required to calculate ε_{eff}. As an example, $\Delta h = 1.524$ mm and $n = 0.1$ gives N = 15 and this implies that the loop in Fig. 3 will run 15 times and modified Δh for which the model calculates ε_{eff} is $0.1*15 = 1.5$ mm instead of 1.524mm. Similarly, N = 16 for $\Delta h = 1.575$mm and $n = 0.1$ and therefore ε_{eff} is determined for modified $\Delta h = 1.6$ mm. Apparently, the model may underestimate or overestimate ε_{eff} based on Δh. However, it will be shown later that this difference is very less and does not have a significant impact.

Step 4: Initialize counter, i. The permittivity of the substrate, ε_1, gets updated in each loop. As a starting point $\varepsilon_i = \varepsilon_1$. Just for clarity, ε_i for i = 1, 2 …N should not be confused with permitivities of substrate and superstrates.

Step 5: Use (10)-(12) to compute ε_{eqs} and ε_{eff}. Reassign ε_1 to newly computed ε_{eff}. In this model, open end extension of the patch is modelled in the form of fringing length ΔL and is taken into account appropriately [24].

TABLE 1. Physical and electrical parameters of the antenna, and feed line designed on RO4350B.

Antenna para.	Value	Antenna para.	Value	Antenna para.	Value
L (mm)	31.5	Patch Impedance	283 Ω	Length of λ/4 line (mm)	17
W (mm)	41.3	Quarter-wave transformer (λ/4) impedance	119 Ω	Width of primary feed (50 Ω) line (mm)	3.6
Effective permittivity	3.34	Width of λ/4 line (mm)	0.5	Length of 50Ω line (mm)	6

Step 6: Determine f_r of the MPA using (13) [7].

$$f_r = \frac{c}{2\,(L + \Delta L)\,\sqrt{\varepsilon_{\text{eff}}}} \tag{13}$$

Step 7: Use (14) to determine the percentage variation between the simulated and theoretically computed f_r.

$$\%var. = \frac{|f_r(\text{Sim.}) - f_r(\text{Th.})|}{f_r(\text{Sim.})} \tag{14}$$

Step 8: It is a conditional check. If i ≤ N then the counter is incremented by i = i+1 else the loop breaks which indicates completion of all steps.

Following aspects are kept in perspectives in the aforementioned steps:

- For the proposed model, h_2' remains constant as it depends on two fixed quantities h and n.
- The frequency dispersion generally decreases for wider conductor (here patch), hence it has not been considered in this model.

IV. ANALYSIS FOR SINGLE SUPERSTRATE LAYER

Extensive simulation using CST has been carried out for MPA covered with single dielectric layer. For this purpose, an MPA is designed on RO4350B with permittivity of 3.66 and thicknesses of 1.524mm. The physical and electrical parameters of the MPA determined by standard expressions in [7] are given in Table 1. A quarter wave transformer matching is used to feed the patch of the MPA with a primary feed line of 50Ω. The electrical and physical parameters of the line are also given in Table 1.

A. SINGLE LAYER OF DIELECTRIC OVER MPA

The designed MPA is covered by superstrate layers, RO4350B, RO5880 ($\varepsilon_2 = 2.2$) and FR4 ($\varepsilon_2 = 4.7$) in such a way that all the conditions $\varepsilon_1 = \varepsilon_2$(case 1), $\varepsilon_1 > \varepsilon_2$(case 2), and $\varepsilon_1 < \varepsilon_2$(case 3) are met. It is important to mention that the formulations derived in this paper are applicable for materials with higher permittivity as well but in this paper superstrate with maximum permittivity of 4.7 is considered to facilitate the in-house fabrication.

The theoretical and simulated results for all the three cases up to the height of 4.5mm are given in Tables 2–4. These tables also provide results obtained from two seminal CM based techniques [19]–[20]. The reason for comparing the proposed work with only [19]–[20] is due to the fact that both these works are considered seminal. Moreover, other reports also make use of the scenarios in these papers and employ the reported expressions in them. The results in Tables 2–4 enable following inferences:

- The proposed model achieves superior performance in terms of relative error in comparison to [19]–[20]. However, for case 2, the % variation is higher for $\Delta h = 4.5$mm w.r.t. [19]. Apparently, for a superstrate of $\varepsilon_2 \leq 2.2$ and smaller heights (1mm – 3mm) the proposed model and the formulation determines ε_{eff} and f_r with better accuracy, but it decreases for larger height.
- First and second rows of Tables 2 and 4 convey that the % variation for the reported technique goes slightly out of pattern. A careful obseravtion of (14) and the values in Tables 2 and 4 agree to the fact that it increases from more negative value to more positive.
- The earlier CM based models [19]–[20] determine ε_{eff} through closed form expressions whereas the proposed model is iterative. But it is still fair to compare the obtained results because the proposed model uses modifed closed form expressions at each iteration. The only difference from the earlier tecniques is that the initial value of substrate permittivity in the proposed model gets updated after each iteration.

It is important to mention here that though frequency dispersion has not been taken into account for the proposed approach and [19]–[20], still the proposed approach outperforms these two.

B. SINGLE LAYER OF TEXTILE OVER MPA

The antenna in wearable sensor has to send data through multiple layers of textile such as cotton, rayon, polyester, wool. Often there may be combination of textiles such as woolen jacket over cotton, felt jacket over polyester and many more. Therefore, textile layers in this analysis is divided in two sets. The first set of textile are immediately next to MPA and comprises of cotton, rayon, and polyester whereas the second set of layer next to first layer is often wool and felt fabric (hoodie). This section limits the analysis for MPA (designed on RO4350B) covered by single layer of textiles as superstrate. The Table 5 lists f_r for the MPA covered with some common textiles both for the proposed model and other CM based models [19]–[20]. The thickness of the textile layers has been taken from earlier reports [25]–[26]. For thinner superstrates (0.2–0.3 mm), it is apparent that the variation in f_r using the proposed technique is mush smaller when compared to well-known CM based techniques [19]–[20]. However, for the thicker superstrates (1–1.5 mm), the variation in f_r increases when compared to [19]. These results are consistent with the outcome in Table 3 and therefore it can be inferred that the variation in f_r is very low for superstrates with $\varepsilon_2 \leq 2.2$ and smaller height when compared to [19]–[20]. However, the variations in f_r for superstrates

TABLE 2. Comparison of simulated and theoretically obtained resonant frequencies of the MPA in this work with [19] and [20] for superstrate of permittivity $\varepsilon_2 = 3.66$ (Case 1: $\varepsilon_1 = \varepsilon_2$) [$\Delta h = h_2 - h$, $L = 31.5$ mm, $W = 41.3$ mm, $\varepsilon_1 = 3.66$, $h_1 = 1.524$ mm at 2.38].

Δh (mm)	ε_{eff} [19]	ε_{eff} [20]	ε_{eff} [Prop.]	Sim. Freq. (GHz) (CST)	Th. Freq. (GHz) [19]	Th. Freq. (GHz) [20]	Th. Freq. (GHz) [Prop.]	%var. [19]	%var. [20]	%var. [Prop.]
1.0	3.6033	3.5010	3.8385	2.317	2.401	2.434	2.338	3.61	5.05	0.91
1.5	3.6281	3.5148	3.9189	2.305	2.392	2.429	2.312	3.80	5.40	0.30
3.0	3.6932	3.5430	4.1277	2.284	2.372	2.421	2.268	3.86	5.95	0.70
4.5	3.7485	3.5616	4.3006	2.270	2.358	2.414	2.230	3.88	6.34	1.76

TABLE 3. (Case 2: $\varepsilon_1 > \varepsilon_2$, where $\varepsilon_1 = 3.66$, and $\varepsilon_2 = 2.2$) (Note: Th. and Prop. signifies theoretical value and proposed method).

Δh (mm)	ε_{eff} [19]	ε_{eff} [20]	ε_{eff} [Prop.]	Sim. Freq. (GHz) (CST)	Th. Freq. (GHz) [19]	Th. Freq. (GHz) [20]	Th. Freq. (GHz) [Prop.]	%var. [19]	%var. [20]	%var. [Prop.]
1.0	3.5966	3.4742	3.8352	2.347	2.403	2.443	2.336	2.40	4.10	0.45
1.5	3.6190	3.4805	3.9147	2.341	2.395	2.441	2.320	2.32	4.27	1.20
3.0	3.6772	3.4936	3.9887	2.330	2.377	2.437	2.292	2.06	4.62	1.58
4.5	3.7257	3.5023	4.1711	2.316	2.362	2.434	2.243	1.82	4.90	3.15

TABLE 4. (Case 3: $\varepsilon_1 < \varepsilon_2$, where $\varepsilon = 3.66$, and $\varepsilon_2 = 4.7$).

Δh (mm)	ε_{eff} [19]	ε_{eff} [20]	ε_{eff} [Prop.]	Sim. Freq. (GHz) (CST)	Th. Freq. (GHz) [19]	Th. Freq. (GHz) [20]	Th. Freq. (GHz) [Prop.]	%var. [19]	%var. [20]	%var. [Prop.]
1.0	3.6058	3.5192	3.8388	2.305	2.400	2.428	2.328	4.12	5.34	1.00
1.5	3.6315	3.5381	3.9196	2.287	2.391	2.422	2.305	4.57	5.89	0.77
3.0	3.6996	3.5766	4.1307	2.260	2.370	2.409	2.250	4.87	6.60	0.44
4.5	3.7581	3.6019	4.3017	2.242	2.352	2.401	2.210	4.92	7.10	1.43

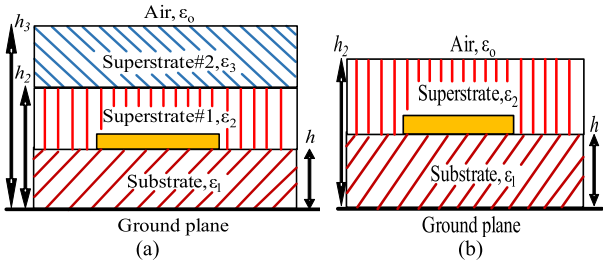

FIGURE 4. a) MPA covered with two superstrate layers, b) Fragmentation of the MPA covered by two dielectric layers to one layer.

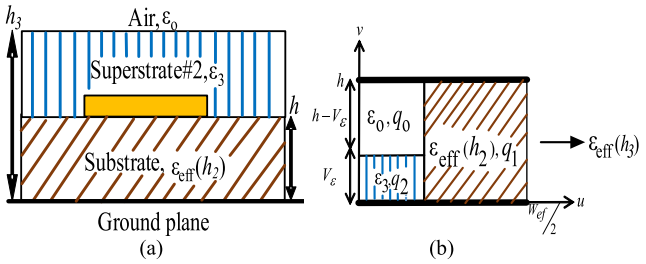

FIGURE 5. (a) MPA covered with second superstrate layer, (b) Approx. of dielectric boundaries with modified. permittivities.

with similar permittivity and larger height is higher for the proposed technique when compared to CM based technique in [19] and this is useful for multi-layer covering of MPA discussed in section V.

V. MODEL FOR TWO SUPERSTRATE LAYERS

The Fig. 4(a) depicts a scenario of MPA covered by two dielectric layers namely superstrate#1 and 2. The height and permittivity of the additional dielectric layer is $\Delta h_1 = h_3 - h_2$ and ε_3. The technique presented here is an extension of the concept where a MPA is covered with single dielectric layer.

A. TWO SUPERSTRATE LAYERS OVER MPA

The determination of ε_{eff} of the structure in Fig. 4(a) consists of two steps. First, fragmentation of two superstrate layers over the MPA as depicted in Fig. 4(b). Then $\varepsilon_{eff}(h_2)$ is computed using the proposed model in section III. Then, the fragmented dielectric layer is restored over the MPA as shown in Fig. 5(a) and the $\varepsilon_{eff}(h_3)$ is computed. The key point in the second step is that the term ε_1 is replaced by $\varepsilon_{eff}(h_2)$, and this scenario is depicted in Fig. 5(b), before using the single layer model formulations. Figs. 4 and 5(a) convey that ε_{eff} for the first superstrate becomes permittivity of the substrate in the second step.

Following additional steps in conjunction with flowchart in Fig. 3 are required to determine ε_{eff} (h_3).

- Choose Δh_1 and ε_3 of the second superstrate layer. First, determine 'n' which might be different from the first superstrate. However, it has been identified that if the values of permittivities of the first and second

TABLE 5. Comparison of simulated and theoretically obtained resonant frequencies of the MPA covered by different textile layers as superstrate in this work with [19] and [20].

Material	ε_2	Δh (mm)	ε_{eff} [19]	ε_{eff} [20]	ε_{eff} [Prop.]	Sim. Freq. (GHz) (CST)	Th. Freq. (GHz) [19]	Th. Freq. (GHz) [20]	Th. Freq. (GHz) [Prop.]	%var. [19]	%var. [20]	%var. [Prop.]
Polyester	**1.40**	0.3	3.557	3.455	3.714	2.372	2.4081	2.4424	2.3655	1.52	3.00	0.27
Jeans	**1.60**	0.3	3.558	3.456	3.714	2.373	2.4077	2.4420	2.3620	1.50	2.91	0.46
Pure cotton	**1.70**	0.2	3.554	3.455	3.697	2.374	2.4092	2.4420	2.3670	1.48	2.86	0.29
Rayon	**3.20**	0.2	3.558	3.465	3.698	2.365	2.4080	2.4380	2.3635	1.82	3.09	0.06
Felt fabric	**1.22**	1.5	3.604	3.455	3.910	2.363	2.3976	2.4422	2.3007	1.46	3.35	2.64
Terry wool	**1.30**	1.5	3.606	3.457	3.907	2.358	2.3922	2.4415	2.3005	1.45	3.54	2.44
Leather	**1.30**	1.5	3.613	3.470	3.913	2.353	2.3902	2.4382	2.3000	1.58	3.62	2.25

superstrates are close then the results do not show significant variation in f_r and therefore n can be kept identical to that used for superstrate 1.

- Determine number of steps M given by M = round $(\Delta h_1/n)$ to calculate ε_{eff} (h_3).
- Initialize another loop with counter j after the determination of ε_{eff} (h_2). As a starting point, assign $\varepsilon_j = \varepsilon_{eff}(h_2)$. Thus, the permittivity of substrate in the i^{th} loop gets updated with ε_{eff} (h_2) as depicted in Fig. 5b. Furthermore, (3)–(12) also gets modified by replacing h_2, ε_1, and ε_2 by h_3, ε_{eff} (h_2), and ε_3 respectively.
- Perform a conditional check of j $\leq$ M at the end of the loop to increment the counter by j+1. If j $\leq$ M, the loop continues else the loop breaks and gives ε_{eff} (h_3).

The above process enables the determination of ε_{eff} and f_r of MPA covered with two superstrate layers. Number of case studies such as $\varepsilon_1 = \varepsilon_2 > \varepsilon_3$, $\varepsilon_1 = \varepsilon_2 < \varepsilon_3$, $\varepsilon_1 < \varepsilon_2 > \varepsilon_3$, $\varepsilon_1 > \varepsilon_2 < \varepsilon_3$, and $\varepsilon_1 > \varepsilon_2 > \varepsilon_3$ are studied as they include all the possible combination of substrate and superstrate. For the cases 1-4, the substrate is RO4350B while the superstrate layer varies from RO5880 to FR4. Therefore, the MPA for the cases 1-4 are designed using the parameters in Table 1. For the case 5, the MPA is designed on FR4 using the new parameters of the antenna and feed line given in Table 6. Tables 7-11 lists the value of ε_{eff} and f_r of all the cases mentioned above and the results are elaborated below.

- The tables list ε_{eff} and f_r for three different heights of superstrate#1 and 2. For example, MPA covered with second superstrate of Δh_1 = 1mm, the ε_{eff} and f_r are calculated for Δh of 1, 1.5, and 2.5mm. Similarly for Δh_1 = 1.5mm and Δh_1 = 2.5mm.
- Apparently, the variation in f_r obtained from the proposed model is much lower when compared to the model in [21]. Finally it can be inferred that the variation in f_r for the proposed model is lower than 2% for overall cover thickness of 5mm over the MPA.
- The variation gradually increases for the proposed model for a given Δh and Δh_1 and it appears, Tables 9 and 11, that the variation has no pattern. But, in reality the simulated and theoretical f_r varies from more negative value to more positive and hence the pattern.

TABLE 6. Physical and electrical parameters of the antenna and feed line designed on FR4.

Antenna para.	Value	Antenna para.	Value	Antenna para.	Value
L (mm)	27.7	Patch Impedance	281 Ω	Length of λ/4 line (mm)	15.8
W (mm)	38.5	Quarter-wave transformer (λ/4) impedance	118 Ω	Width of primary feed (50 Ω) line (mm)	2.8
Effective permittivity	3.946	Width of λ/4 line (mm)	0.37	Length of 50Ω line (mm)	5.6

B. TWO TEXTILE LAYERS OVER MPA

The designed MPA on RO4350B is taken as a source of EM wave. Subsequently, it is covered by combinations of textile layers mentioned in Table 12 to analyze the proposed technique. Layer 1 consist of textiles which are next to MPA such as pure cotton, jeans cotton, rayon and polyester. Layer 2 consist of textile which are worn over the layer 1 in real life such as woolen jackets and hoodies made of felt. The approach adopted here makes use of the technique proposed for single superstrate in this paper and an earlier method [19] to determine f_r and ε_{eff} for such arrangements. It is done to overcome the specific limitations of the proposed technique whenever the % variation is higher when compared to the earlier approach [19] for covers like wool and felt (layer 2) as can be seen in Table 5. The idea here is to first determine ε_{eff} (h_2) that constitutes layer 1 over MPA using the proposed technique. The arrangement over the MPA then reduces to one superstrate layer after the determination of ε_{eff} (h_2) and depicts the scenario shown in Fig. 5a.

Subsequently, in the next step, ε_1 is replaced with ε_{eff} (h_2) and then ε_{eff} (h_3) is determined for a given Δh_1 by employing the technique in [19]. The obtained results are given in Table 12. It should be noted that the thickness of layer 1 in Tables 5 and 12 is limited to 0.2–0.4 mm considering the practical scenarios/applications. However, woolen and felt jackets are in general thick and therefore the thickness of 1–1.5 mm are used in the analysis. It is clear that the variations

TABLE 7. Comparison of simulated and theoretically obtained resonant frequencies of the MPA covered by two superstrate layers in this work with [21] (Case 1: $\varepsilon_1 = \varepsilon_2 < \varepsilon_3$, where $\varepsilon_1 = \varepsilon_2 = 3.66$, and $\varepsilon_3 = 4.7$) [$\Delta h_1 = h_3 - h_2$, $\Delta h = h_2 - h_1$, L= 31.5 mm, W= 41.3 mm].

Δh_1 (mm)	Δh (mm)	ε_{eff} [21]	$\varepsilon_{eff}(h_2)$ [Prop.]	$\varepsilon_{eff}(h_3)$ [Prop.]	Sim. Freq. (GHz) (CST)	Th. Freq. (GHz) [21]	Th. Freq. (GHz) [Prop.]	%var. [21]	%var. [Prop.]
1.0	1.0 1.5 2.5	3.527	3.838 3.919 4.064	3.995	2.302	2.393	2.300	3.95	0.08
		3.544		4.056	2.296	2.387	2.280	3.96	0.70
		3.579		4.191	2.283	2.376	2.245	4.07	1.66
1.5		3.533		4.044	2.290	2.391	2.288	4.41	0.09
		3.551		4.120	2.285	2.385	2.267	4.47	0.78
		3.587		4.240	2.272	2.373	2.234	4.49	1.67
2.5		3.545		4.140	2.270	2.387	2.260	5.15	0.44
		3.564		4.222	2.262	2.381	2.240	5.26	0.97
		3.602		4.343	2.250	2.368	2.210	5.43	1.70

TABLE 8. (Case 2: $\varepsilon_1 = \varepsilon_2 > \varepsilon_3$, where $\varepsilon_1 = \varepsilon_2 = 3.66$, and $\varepsilon_3 = 2.2$).

Δh_1 (mm)	Δh (mm)	ε_{eff} [21]	$\varepsilon_{eff}(h_2)$ [Prop.]	$\varepsilon_{eff}(h_3)$ [Prop.]	Sim. Freq. (GHz) (CST)	Th. Freq. (GHz) [21]	Th. Freq. (GHz) [Prop.]	%var. [21]	%var. [Prop.]
1.0	1.0 1.5 2.5	3.508	3.838 3.919 4.064	3.988	2.314	2.400	2.305	3.72	0.40
		3.519		4.058	2.305	2.396	2.286	3.94	0.82
		3.538		4.170	2.284	2.390	2.255	4.64	1.27
1.5		3.511		4.038	2.311	2.398	2.291	3.77	0.87
		3.522		4.120	2.300	2.395	2.270	4.13	1.30
		3.542		4.211	2.282	2.388	2.243	4.70	1.70
2.5		3.517		4.152	2.300	2.396	2.264	4.17	1.70
		3.528		4.225	2.286	2.393	2.246	4.68	1.75
		3.548		4.301	2.262	2.386	2.222	5.48	1.80

achieved by the combined technique is significantly lower when compared to the approach reported in [21].

VI. MEASURED RESULTS

Two MPAs, given in Figs. 6(a) and (b), operating at 2.38 GHz using parameters in Tables 1 and 6 are prototyped to validate the presented theory. The dielectric layers RO4350B, RO5880, and FR4 to be used as superstrate of identical size are also fabricated. The successive layers of the superstrates are positioned one after another and stacked together over the MPA with the help of low permittivity adhesive RTV coating ($\varepsilon_r = 1.22$). For the MPA covered with textiles, measurement of f_r in VNA is carried out by placing either single or multiple layers over it. The results in the form of plot is given for some cases while the detailed results are provided in tables.

A. SINGLE SUPERSTRATE AND TEXTILE OVER MPA

The measurement for the first two rows of Table 2 are shown in Figs. 7(a)-(b). The MPA covered with a single layer of RO4350B of $h = 1.524$mm is given in Fig. 7(a) whereas measurement of MPA covered with two layers of RO4350B having combined height of 3.048mm is depicted in Fig. 7(b). It is important to take care while applying the adhesive (RTV coating) on the dielectric layer so that no air gap is formed

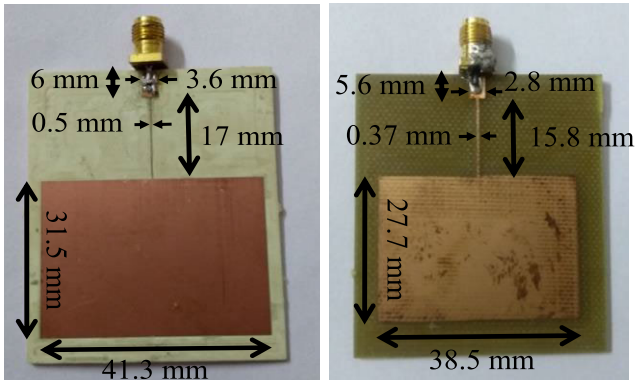

FIGURE 6. (a) Prototyped MPA on RO4350B (b) Prototyped MPA on FR4.

at the interface. Moreover, sufficient space is left at the feed location to suitably place the dielectric layers over the MPA in the presence of SMA connectors in both Figs. 7(a)-(b). The plot in Fig. 7(c) depicts measured f_r of uncovered along with superstrate covered MPA for all the thicknesses mentioned in Table 13. The selection of Δh in Tables 13–15 are regulated by the availability of resources for in-house fabrication. Moreover, the values of Δh in Tables 13–15 for measurement of f_r may differ from the values used for the determination of theoretical f_r. For example, for $\Delta h = 1.524$mm, the step III of

TABLE 9. (Case 3: $\varepsilon_1 < \varepsilon_2 > \varepsilon_3$, where $\varepsilon_1 = 3.66$, $\varepsilon_2 = 4.7$ and $\varepsilon_3 = 2.2$).

Δh_1 (mm)	Δh (mm)	ε_{eff} [21]	$\varepsilon_{eff}(h_2)$ [Prop.]	$\varepsilon_{eff}(h_3)$ [Prop.]	Sim. Freq. (GHz) (CST)	Th. Freq. (GHz) [21]	Th. Freq. (GHz) [Prop.]	%var. [21]	%var. [Prop.]
1.0	1.0	3.511	3.840	3.990	2.295	2.398	2.302	4.50	0.35
		3.523		4.055	2.285	2.394	2.284	4.77	0.04
		3.546		4.190	2.264	2.387	2.250	5.43	0.62
1.5	1.5	3.515	3.921	4.058	2.294	2.397	2.284	4.50	0.44
		3.527		4.120	2.282	2.393	2.270	4.86	0.53
		3.550		4.244	2.262	2.385	2.235	5.44	1.20
2.5	2.5	3.520	4.067	4.160	2.285	2.395	2.258	4.81	1.18
		3.533		4.211	2.276	2.391	2.244	5.05	1.41
		3.557		4.330	2.253	2.383	2.215	5.77	1.68

TABLE 10. (Case 4: $\varepsilon_1 > \varepsilon_2 < \varepsilon_3$, where $\varepsilon_1 = 3.66$, $\varepsilon_2 = 2.2$ and $\varepsilon_3 = 4.7$).

Δh_1 (mm)	Δh (mm)	ε_{eff} [21]	$\varepsilon_{eff}(h_2)$ [Prop.]	$\varepsilon_{eff}(h_3)$ [Prop.]	Sim. Freq. (GHz) (CST)	Th. Freq. (GHz) [21]	Th. Freq. (GHz) [Prop.]	%var. [21]	%var. [Prop.]
1.0	1.0	3.515	3.833	3.987	2.332	2.397	2.330	2.80	0.09
		3.527		4.068	2.323	2.393	2.306	3.01	0.73
		3.550		4.160	2.312	2.385	2.280	3.16	1.38
1.5	1.5	3.521	3.925	4.056	2.320	2.395	2.310	3.23	0.43
		3.533		4.135	2.315	2.391	2.287	3.28	1.18
		3.556		4.230	2.305	2.383	2.267	3.38	1.60
2.5	2.5	3.531	4.053	4.172	2.311	2.392	2.288	3.50	1.00
		3.543		4.251	2.302	2.388	2.266	3.73	1.55
		3.567		4.324	2.292	2.380	2.250	3.84	1.80

the proposed model determines ε_{eff} and f_r for the modified Δh of 1.5mm. Similarly, theoretical f_r are determined for modified Δh of 3, 4.6, 1.6, 3.2 and 4.7mm for the respective $\Delta h =$ 3.048, 4.572, 1.575, 3.15, and 4.725mm. As a consequence, the proposed underestimates or overestimates the eventual ε_{eff} and f_r. But it is apparent from the data in Tables 13-15 that the measured/simulated and theoretical results show excellent agreement despite the presence of slight anomaly in the selection of Δh.

To evaluate the proposed technique for practical applications such as on-body communication, similar steps for measuring f_r of MPA covered with single felt fabric layer is developed as shown in the measurement setup of Fig. 8(a). During the measurement with textiles, formation of air gap between its layer and MPA is avoided by taking appropriate care. For this, a layer of textile is pressed over the MPA with cosiderable force at the bottom. Therefore, this work restricts its analysis to textiles over MPA without air gap. However, in the presence of SMA connector and cable, buldge appears due to air gap as can be seen in Fig. 8(a). This air gap, however, has very little impact considering that majority of the radiation takes place near the patch which is well covered by the textile layer. The measured results for all the textile layers, given in Table 16, show very good agreement with the theoretical values in Table 5. In addition, the measured values of f_r in Fig. 8(b) for the MPA covered with wool, jeans cotton, and polyester with the respective Δh of 1.5, 0.3, and 0.3 mm clearly show that these are very close with that of theoretical values.

B. EFFECTIVENESS OF THE PROPOSED MODEL TO RESTORE f_r

The original f_r can be restored by altering the length once the ε_{eff} for a given superstrate over the MPA is determined. For this, the determined ε_{eff} from the proposed model becomes the new permittivity of the design to recalculate new physical parameters of the MPA. The condition in row 3 of the Table 2 is used to elaborate this aspect. For the parameters in the Table 2, the ε_{eff} is 4.1277 and this is used to compute the modified length of the MPA. In order to restore the original f_r i.e. 2.38GHz, the modified length is given by (15). Here, L^m is the modified length of the MPA.

$$f_r = \frac{c}{2\,(L^m + \Delta L)\,\sqrt{\varepsilon_{eff}}} \tag{15}$$

The substitution of known values of f_r, ε_{eff}, c, and ΔL in (15) results in L^m of 29.37mm. The MPA resonates at 2.392GHz, as depicted in Fig. 7(c), for the newly computed length. The shift in frequency from the original can be attributed to the overestimation of ε_{eff} by the model. This implies that for the chosen case, the obtained f_r from the model is lower than the simulated f_r as is evident from Table 2 due to overestimation of ε_{eff}. Apparently, substitution of this ε_{eff} in (15) results in smaller L^m than the desired length

TABLE 11. (Case 5: $\varepsilon_1 > \varepsilon_2 > \varepsilon_3$, where $\varepsilon_1 = 4.7$, $\varepsilon_2 = 3.66$ and $\varepsilon_3 = 2.2$) ($L = 27.7$ mm, $W = 38.5$ mm).

Δh_1 (mm)	Δh (mm)	ε_{eff} [21]	$\varepsilon_{eff}(h_2)$ [Prop.]	$\varepsilon_{eff}(h_3)$ [Prop.]	Sim. Freq. (GHz) (CST)	Th. Freq. (GHz) [21]	Th. Freq. (GHz) [Prop.]	%var. [21]	%var. [Prop.]
1.0	1.0	4.471	4.803	4.895	2.317	2.391	2.330	3.20	0.56
		4.482		4.937	2.308	2.388	2.320	3.47	0.52
		4.503		5.021	2.292	2.383	2.300	4.00	0.35
1.5	1.5	4.475	4.850	4.942	2.312	2.390	2.318	3.37	0.26
		4.486		4.976	2.305	2.387	2.311	3.56	0.25
	2.5	4.507	4.938	5.056	2.290	2.382	2.293	4.02	0.13
2.5		4.481		5.003	2.310	2.388	2.298	3.38	0.52
		4.492		5.050	2.300	2.386	2.288	3.74	0.53
		4.512		5.124	2.285	2.380	2.269	4.16	0.70

TABLE 12. Comparison of simulated and theoretically obtained resonant frequencies of the MPA covered by two textile layers as superstrate layers in this work with [21].

Layer 1	Layer 2	Δh (mm)	Δh_1 (mm)	ε_{eff} [21]	$\varepsilon_{eff}(h_2)$ [Prop.]	$\varepsilon_{eff}(h_3)$ [Prop.]	Sim. Freq. (GHz)	Th. Freq. (GHz) [21]	Th. Freq. (GHz) [Prop.]	%var. [21]	%var. [Prop.]
Polyester	Terry wool	0.2	1.0	3.471	3.696	3.622	2.368	2.4119	2.387	1.85	0.80
			1.5	3.472		3.642	2.367	2.4116	2.381	1.88	0.60
		0.3	1.0	3.472	3.714	3.640	2.365	2.4116	2.382	1.97	0.72
			1.5	2.473		3.660	2.364	2.4113	2.375	2.00	0.46
Jeans cotton	Terry wool	0.3	1.0	2.473	3.716	3.641	2.365	2.4112	2.381	1.95	0.68
			1.5	3.474		3.663	2.362	2.4109	2.375	2.06	0.55
		0.4	1.0	3.474	3.732	3.660	2.362	2.4109	2.376	2.06	0.60
			1.5	3.475		3.678	2.360	2.4105	2.370	2.14	0.42
Pure cotton	Felt	0.2	1.0	3.471	3.697	3.622	2.368	2.4118	2.387	1.85	0.80
			1.5	3.472		3.642	2.365	2.4115	2.381	1.97	0.68
		0.3	1.0	3.472	3.715	3.640	2.365	2.4115	2.381	1.97	0.68
			1.5	3.473		3.660	2.362	2.4112	2.375	2.08	0.55
Rayon	Felt	0.2	1.0	3.475	3.700	3.623	2.362	2.4104	2.387	2.05	1.06
			1.5	3.476		3.644	2.358	2.4102	2.380	2.21	0.93
		0.3	1.0	3.477	3.726	3.641	2.356	2.410	2.381	2.30	1.06
			1.5	2.478		3.670	2.350	2.4096	2.375	2.54	1.05

TABLE 13. Comparison of measured and theoretically obtained resonant frequencies of the MPA for superstrate of permittivity $\varepsilon_2 = 3.66$ (case 1: $\varepsilon_1 = \varepsilon_2$).

Δh (mm)	Meas. Freq. (GHz)	%var. [19]	%var. [20]	%var. [Prop.]
1.524	2.302	3.55	5.15	0.43
3.048	2.290	3.42	5.50	0.96
4.572	2.262	4.25	6.80	1.85

TABLE 14. Comparison of measured and theoretically obtained resonant frequencies of the MPA for superstrate of permittivity $\varepsilon_2 = 2.2$ (case 2: $\varepsilon_1 > \varepsilon_2$).

Δh (mm)	Meas. Freq. (GHz)	%var. [19]	%var. [20]	%var. [Prop.]
1.575	2.338	2.40	4.40	1.25
3.150	2.327	2.06	4.70	1.80
4.725	2.312	2.00	5.23	3.24

TABLE 15. Comparison of measured and theoretically obtained resonant frequencies of the MPA for superstrate of permittivity $\varepsilon_2 = 4.7$ (case 3: $\varepsilon_1 < \varepsilon_2$).

Δh (mm)	Meas. Freq. (GHz)	%var. [19]	%var. [20]	%var. [Prop.]
1.5	2.290	4.41	5.76	0.66
3.0	2.262	4.80	6.50	0.53
4.5	2.245	4.80	6.95	1.56

to bring resonance at 2.38 GHz. Thus it can be inferred that the smaller variation leads to higher accuracy in the determination of L^m and hence better accuracy in the restoration of the original f_r. It is imperative to note that only the length in the above discussion is modified while keeping the width unchanged and as a result the return loss is poor as can be seen in Fig. 7(c).

C. TWO SUPERSTRATE AND TEXTILE OVER MPA

The f_r for the combination of superstrates, listed in Tables 7–11, over the MPA are measured. The measurement setup with successive layers of superstrates over the MPA is similar to Fig. 7(a)-(b) with the only difference being the stacking of distinct second layer. The measurement results for some of the Δh_1 and Δh covering all five cases in section V

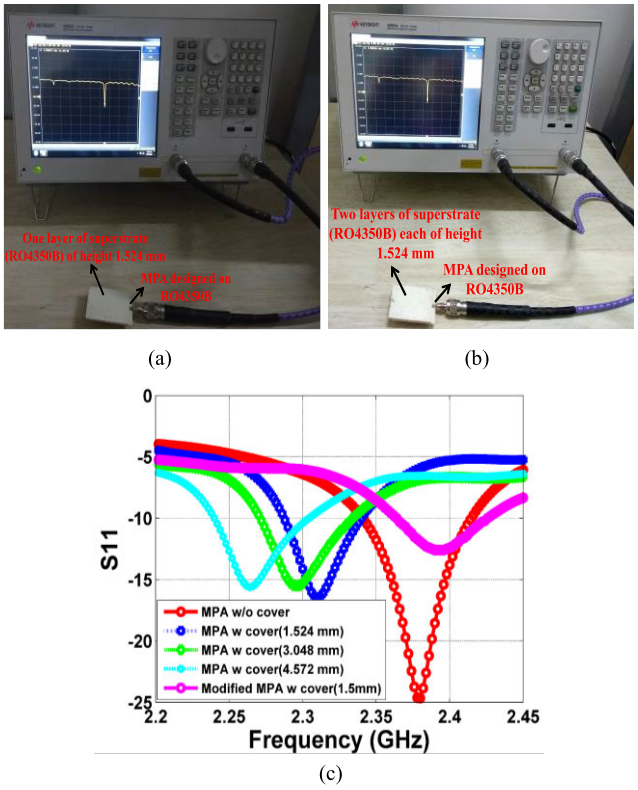

FIGURE 7. (a) Measurement setup of fabricated prototype on RO4350 substrate and superstrate for $\Delta h = 1.524$ mm exhibiting f_r of 2.302 GHz (b) $\Delta h = 3.048$mm exhibiting f_r of 2.29 GHz (c) Return loss of MPA on RO4350B with and without cover of $\Delta h = 1.524$, 3.048, and 4.572 mm.

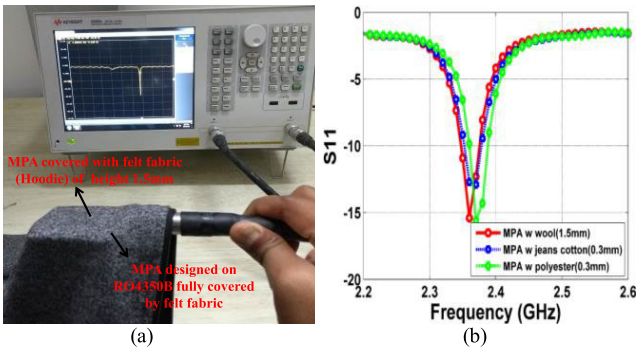

FIGURE 8. (a) Measurement setup of MPA covered with felt fabric (hoodie) (b) Return loss of MPA covered with wool, jeans cotton and polyester with $\Delta h = 1.5$, 0.3, and 0.3 mm.

are given in Table 17. An MPA on FR4 substrate is prototyped for the parameters given in Table 6 to measure case 5 of Table 17. Apparently, the variations in f_r are in good agreement with the predicted values in section V. This validates the effectiveness of the proposed model for two dielectric layers over the MPA.

Subsequently, the MPA is covered with the combination of textile layers mentioned in Table 12 and the values of f_r are measured using the setup given in Fig. 8(a). The Table 18 includes the measured f_r for some of the combinations. The chosen thickness of the textile layers in this work

TABLE 16. Comparison of measured and theoretically obtained resonant frequencies of the MPA covered with single textile superstrates.

Material	ε_2	Δh^* (mm)	Meas. Freq. (GHz)	%var. [19]	%var. [20]	%var. [Prop.]
Polyester	1.40	0.3	2.375	1.46	2.84	0.40
Jeans cotton	1.60	0.3	2.373	1.50	2.91	0.46
Pure cotton	1.70	0.2	2.371	1.61	3.00	0.17
Rayon	3.20	0.2	2.367	1.73	3.00	0.15
Felt fabric	1.22	1.5	2.363	1.46	3.35	2.64
Terry wool	1.30	1.5	2.358	1.45	3.54	2.44
Leather	1.66	1.5	2.359	1.32	3.36	2.50

TABLE 17. Comparison of measured and theoretically obtained resonant frequencies of the MPA covered with two superstrate layers.

Case	Δh_1 (mm)	Δh (mm)	Meas. Freq. (GHz)	%var. [21]	%var. [Prop.]
$\varepsilon_1 = \varepsilon_2 < \varepsilon_3$	1.500	1.524	2.286	4.33	0.83
$\varepsilon_1 = \varepsilon_2 > \varepsilon_3$	1.575	1.524	2.302	4.04	1.40
$\varepsilon_1 < \varepsilon_2 > \varepsilon_3$	1.575	1.500	2.290	4.50	0.87
$\varepsilon_1 > \varepsilon_2 < \varepsilon_3$	1.500	1.575	2.318	3.15	1.34
$\varepsilon_1 > \varepsilon_2 > \varepsilon_3$	1.575	1.524	2.307	3.47	0.17

TABLE 18. Comparison of measured and theoretically obtained resonant frequencies of the MPA covered with two textile layers.

Layer 1	Layer 2	Δh (mm)	Δh_1 (mm)	Meas. Freq. (GHz)	%var. [21]	%var. [Prop.]
Polyester	Wool	0.3	1.5	2.3708	1.71	0.18
Jeans cotton	Wool	0.3	1.5	2.3628	2.04	0.52
Pure cotton	Felt	0.2	1.5	2.3668	1.85	0.60
Rayon	Felt	0.2	1.5	2.3547	2.33	1.07

is the average of many samples. It is once again clear that the measured variation in f_r perfectly agrees with the predicted values in Table 12 and therefore demonstrate the scalability of the proposed model to two superstrate layers.

D. MULTI-TEXTILE LAYER OVER MPA

Next the effectiveness of the proposed theory for multi-layered superstrate structures over the MPA is demonstrated, using identical measurement to Fig. 8a, with a combination of polyester, foam, and polyester (typically a windcheater). The polyester form layers 1 and 3 whereas layer 2 consists of foam. No air gap between the successive layers in simulation as well as in measurement is considered. The thickness of foam and polyester is takes as 1.2mm and 0.3mm while the corresponding permittivities are 1.13 and 1.4 in both the simulation and measurement scenarios. The presence of third superstrate layer of thickness h_4 makes the parameter $\Delta h_2 = h_4 - h_3$. Then f_r is determined using the steps in sections III and V for the combinations mentioned in Table 19. The comparison between the theoretical, simulated, and measured f_r for the proposed technique

TABLE 19. Comparison of simulated, measured and theoretically obtained resonant frequencies of the MPA covered by three textile layers as superstrate (Wind Cheater) in this work with [21].

Lay 1	Lay 2	Lay 3	Δh (mm)	Δh_1 (mm)	Δh_2 (mm)	Sim. Freq. (GHz)	Meas. Freq. (GHz)	Th. Freq. (GHz) [21]	Th. Freq. (GHz) [Prop.]	%var. [21] (Sim.)	%var. [Prop.] (Sim.)	%var. [21] (Mea.)	%var. [Prop.] (Mea.)
Poly ester	Foam	Poly ester	0.3	1.2	0.3	2.374	2.375	2.410	2.381	1.52	0.30	1.47	0.25

shows excellent consonance. In addition, the variation for the proposed technique is substantially smaller when compared to the results obtained using technique reported in [21]. The obtained results also demonstrate that the proposed model and formulations is scalable with extremely good accuracy to the situations when MPA is covered with multiple layers on it therefore significantly advances the existing state-of-the-art.

VII. CONCLUSION

A novel iterative model along with a new empirical relation to determine ε_{eff} and f_r of MPA covered with multiple dielectric layers is reported in this paper. The formulation of ε_{eff} is based on series–parallel combination of dielectric loaded capacitors between the metallic patch and the ground plane. The estimation of shift in f_r apriori is desired in wireless body area network for achieving desired reliability. It is well accepted that a reliable link to transfer essential physiological parameters to an external node is essential considering that no loss of data should take place due to out-of band communication between transmitter and receiver. To facilitate this, the presented model determines $\varepsilon_{\text{effi}}$ for substrate and the first superstrate layer. The process is then repeated by replacing $\varepsilon_1 = \varepsilon_{\text{effi}}$ for the successive superstrate layers and this ultimately results in ε_{eff} and f_r for the whole structure. The model then determines f_r of MPA covered with single superstrate layer for the three cases of $\varepsilon_1 = \varepsilon_2$, $\varepsilon_1 > \varepsilon_2$ and $\varepsilon_1 < \varepsilon_2$. The small variations in the measured and simulated f_r for the proposed model for the three cases suggest that the model is very good for dielectric cover of $\varepsilon_2 > 2.2$. Furthermore, the proposed model when tested on MPA covered with textile layers shows excellent performance for thinner heights and a slightly weaker performance for thicker superstrates. The application of the proposed model on MPA covered with two superstrate layers for $\varepsilon_1 = \varepsilon_2 > \varepsilon_3$, $\varepsilon_1 = \varepsilon_2 < \varepsilon_3$, $\varepsilon_1 < \varepsilon_2 > \varepsilon_3$, $\varepsilon_1 > \varepsilon_2 < \varepsilon_3$, and $\varepsilon_1 > \varepsilon_2 > \varepsilon_3$ respectively shows outstanding result with lower variations when compared to the state-of-the-art techniques. It is also shown that the proposed model when employed in conjunction with an existing technique significantly advances the state-of-the-art. In brief, the proposed model has lower complexity and therefore has the potential for easy incorporation with any technical computing software.

ACKNOWLEDGMENT

The authors also want to thanks Mrs. Nivedita for her help during the measurement with textiles.

REFERENCES

[1] C. Hill and T. Kneisel, "Portable radio antenna performance in the 150, 450, 800, and 900 MHz bands 'outside' and in-vehicle," *IEEE Trans. Veh. Technol.*, vol. 40, no. 4, pp. 750–756, Nov. 1991.

[2] B. Yildirim, "Multiband and compact WCDMA/WLAN antenna for mobile equipment," *IEEE Antennas Wireless Propag. Lett.*, vol. 10, pp. 14–16, 2011.

[3] P. S. Hall and Y. Hao, *Antennas and Propagation for Body-centric Wireless Communications*, 2nd ed. Norwood, MA, USA: Artech House, 2012.

[4] C. Roblin, J. M. Laheurte, and R. D'Errico, "Antenna design and channel modeling in the BAN context—Part I: Antennas," *Ann. Telecomm.*, vol. 66, no. 3, pp. 139–155, Jan. 2011.

[5] M. Karimyian-Mohammadabadi, M. A. Dorostkar, F. Shokuohi, M. Shanbeh, and A. Torkan, "Super-wideband textile fractal antenna for wireless body area networks," *J. Electromagn. Waves Appl.*, vol. 29, no. 13, pp. 1728–1740, Jul. 2015.

[6] A. Bhattacharyya and T. Tralman, "Effects of dielectric superstrate on patch antennas," *Electron. Lett.*, vol. 24, no. 6, pp. 356–358, 1988.

[7] C. A. Balanis, *Antenna Theory Analysis and Design*, 3rd ed. New York, NY, USA: Wiley, 1997.

[8] W. El Hajj, C. Person, and J. Wiart, "A novel investigation of a broadband integrated inverted-F antenna design; application for wearable antenna," *IEEE Trans. Antennas Propag.*, vol. 62, no. 7, pp. 3843–3846, Jul. 2014.

[9] M. N. Suma, P. C. Bybi, and P. Mohanan, "A wideband printed monopole antenna for 2.4-GHz WLAN applications," *Microw. Opt. Technol. Lett.*, vol. 48, no. 5, pp. 871–873, 2006.

[10] D. Rano and M. Hashmi, "Design and analysis of wearable patch antenna array for MBAN applications," in *Proc. 22nd Nat. Conf. Commun. (NCC)*, Guwahati, India, Mar. 2016, pp. 1–6.

[11] S.-J. Ha, Y.-B. Jung, D. H. Kim, and C. W. Jung, "Textile patch antennas using double layer fabrics for wrist-wearable applications," *Microw. Opt. Technol. Lett.*, vol. 54, no. 12, pp. 2697–2702, Sep. 2012.

[12] I. Bahl, P. Bhartia, and S. Stuchly, "Design of microstrip antennas covered with a dielectric layer," *IEEE Trans. Antennas Propag.*, vol. AP-30, no. 2, pp. 314–318, Mar. 1982.

[13] R. Shavit, "Dielectric cover effect on rectangular microstrip antenna array," *IEEE Trans. Antennas Propag.*, vol. 42, no. 8, pp. 1180–1184, Aug. 1994.

[14] A. K. Verma and Z. Rostamy, "Resonant frequency of uncovered and covered rectangular microstrip patch using modified wolff model," *IEEE Trans. Microw. Theory Techn.*, vol. 41, no. 1, pp. 109–116, Jan. 1993.

[15] J. P. Damiano and A. Papiernik, "A simple and accurate model for the resonant frequency and the input impedance of printed antennas," *Int. J. Microw. Millim.-Wave Comput.-Aided Eng.*, vol. 3, no. 4, pp. 350–361, Oct. 1993.

[16] H. A. Wheeler, "Transmission-line properties of parallel wide strips by a conformal-mapping approximation," *IEEE Trans. Microw. Theory Techn.*, vol. 12, no. 3, pp. 280–289, May 1964.

[17] H. A. Wheeler, "Transmission-line properties of parallel strips separated by a dielectric sheet," *IEEE Trans. Microw. Theory Techn.*, vol. 13, no. 2, pp. 172–185, Mar. 1965.

[18] J. Svacina, "Analysis of multilayer microstrip lines by a conformal mapping method," *IEEE Trans. Microw. Theory Techn.*, vol. 40, no. 4, pp. 769–772, Apr. 1992.

[19] S.-S. Zhong, G. Liu, and G. Qasim, "Closed form expressions for resonant frequency of rectangular patch antennas with multidielectric layers," *IEEE Trans. Antennas Propag.*, vol. 42, no. 9, pp. 1360–1363, Sep. 1994.

[20] J. T. Bernhard and C. J. Tousignant, "Resonant frequencies of rectangular microstrip antennas with flush and spaced dielectric superstrates," *IEEE Trans. Antennas Propag.*, vol. 47, no. 2, pp. 302–308, Feb. 1999.

[21] J. Svacina, "A simple quasi-static determination of basic parameters of multilayer microstrip and coplanar waveguide," *IEEE Microw. Guided Wave Lett.*, vol. 2, no. 10, pp. 385–387, Oct. 1992.
[22] D. Rano and M. S. Hashmi, "Determination of effective dielectric constant and resonant frequency of microstrip patch antenna with multilayered superstrate structures," in *Proc. EuMC*, Paris, France, Oct. 2019, pp. 81–84.
[23] CST, Framingham, MA, USA. (2012). *CST Microwave Studio*. [Online]. Available: http://www.cst.com
[24] M. Kirschning, R. H. Jansen, and N. H. L. Koster, "Accurate model for open end effect of microstrip lines," *Electron. Lett.*, vol. 17, no. 3, pp. 123–125, Feb. 1981.
[25] S. Sankaralingam and B. Gupta, "Determination of dielectric constant of fabric materials and their use as substrates for design and development of antennas for wearable applications," *IEEE Trans. Instrum. Meas.*, vol. 59, no. 12, pp. 3122–3130, Dec. 2010.
[26] J. Tak, J. Choi, and S. Lee, "All-textile higher order mode circular patch antenna for on-body to on-body communications," *IET Microw., Antennas Propag.*, vol. 9, no. 6, pp. 576–584, Apr. 2015.

DINESH RANO (Student Member, IEEE) was born in Dhanbad, India, in 1989. He received the B.Tech. degree from the West Bengal University of Technology (WBUT) and the M.Tech. degree from Jaypee University (JIIT), both in electronics and communication engineering. He is currently pursuing the Ph.D. degree with the Department of Electronics and Communication Engineering, Indraprastha Institute of Information Technology Delhi (IIIT Delhi). His research interests include antenna design for body centric communication, conformal antennas, and generating link-budget for on-body communication. He was a recipient of the prestigious award of Visvesvaraya Fellowship from the Ministry of Human Resource Department (MHRD), India, in August 2015. He also won many prizes as Best Filter Design Contest, Best Report Award, and Student Grant in IMaRC and EUMC.

MUHAMMAD A. CHAUDHARY (Senior Member, IEEE) received the Ph.D. degree in electrical and electronics engineering from Cardiff University, U.K., in September 2011. He completed his doctoral research work at the Agilent Center for High Frequency Engineering, where he was actively involved in the development of novel modulated load-pull measurement setups for power transistor characterization and power amplifier measurements under multitone excitations. He was a Postdoctoral Research Associate at the Agilent Centre for High Frequency Engineering, Cardiff University, from October 2011 to September 2012. In addition to his research activities as a Postdoctoral Research Associate, he carried out commercial work for Freescale Semiconductor, Mesuro, TriQuint Semiconductor, and National Physical Laboratory (NPL) using the Nonlinear Measurement System pioneered at Cardiff University, U.K. He is currently an Associate Professor of electrical engineering at Ajman University. He teaches various courses related to the field of electrical engineering and conducts research in the broad field of microwave engineering. He has authored the book "*Modulated Measurement and Engineering Systems for Microwave Power Transistors*" and authored/coauthored over 53 peer-reviewed articles. He is a Chartered Engineer (CEng), Engineering Council, U.K. For his doctoral studies in radio frequency and microwave electronics, he was granted funding from Engineering and Physical Sciences Research Council (EPSRC).

MOHAMMAD S. HASHMI (Senior Member, IEEE) received the B.Tech. degree from Aligarh Muslim University, India, the M.S. degree from the Darmstadt University of Technology, Germany, and the Ph.D. degree from Cardiff University, Cardiff, U.K. He had held research and engineering positions at the University of Calgary, Canada, Cardiff University, U.K., Thales Electronics GmbH, Germany, and Philips Technology Center, Germany. He is currently an Associate Professor with Nazarbayev University, Kazakhstan, and also holds a faculty position at IIIT Delhi, India. His current research interests are in advanced RF circuits, broadband linear and efficient power amplifiers for mobile and satellite applications, and high- and low-frequency instrumentation. His research activities have led to one book and over 180 journal and conference publications, and holds three U.S. patents (two pending). He is an Associate Editor of the *IEEE Microwave Magazine*.